

**MICROSTRUCTURAL EVOLUTION OF HFIR-IRRADIATED LOW ACTIVATION F82H AND F82H-<sup>10</sup>B STEELS** -- E. Wakai (Japan Atomic Energy Research Institute), N. Hashimoto (Oak Ridge National Laboratory), K. Shiba and T. Sawai (JAERI), and J. P. Robertson and R. L. Klueh (Oak Ridge National Laboratory)

**OBJECTIVE**

The purpose of the present study is to characterize the microstructure of ferritic-martensitic steels following neutron irradiation in the range 200 - 500°C and explore the relationships between mechanical behavior and microstructure.

**SUMMARY**

Microstructures of reduced-activation F82H (8Cr-2W-0.2V-0.04Ta) and the F82H steels doped with <sup>10</sup>B, irradiated at 250 and 300°C to 3 and 57 dpa in the High Flux Isotope Reactor (HFIR), were examined by TEM. In the F82H irradiated at 250°C to 3 dpa, dislocation loops, small unidentified defect clusters with a high number density, and a few MC precipitates were observed in the matrix. The defect microstructure after 300°C irradiation to 57 dpa is dominated by the loops, and the number density of loops was lower than that of the F82H-<sup>10</sup>B steel. Cavities were observed in the F82H-<sup>10</sup>B steels, but the swelling value is insignificant. Small particles of M<sub>6</sub>C formed on the M<sub>23</sub>C<sub>6</sub> carbides that were present in both steels before the irradiation at 300°C to 57 dpa. A low number density of MC precipitate particles formed in the matrix during irradiation at 300°C to 57 dpa.

**PROGRESS AND STATUS**

1. Introduction

Ferritic/martensitic steels are candidate materials for the first wall and blanket structure of fusion reactors. In the D-T fusion reaction, the high-energy neutrons produced induce displacement damage and generate gas atoms in the materials from (n, p) and (n, α) reactions. The presence of these gases could lead to degradation of mechanical properties. The effect of helium atoms generated from the (n, α) reaction can be simulated by using a steel doped with <sup>10</sup>B or <sup>58</sup>Ni and irradiating in a mixed-spectrum fission reactor, such as the High Flux Isotope Reactor (HFIR).

The effect of neutron irradiation on the tensile deformation of alloy F82H has been reported. Shiba et al. [1,2] described the tensile data following irradiation in HFIR at 200 to 600°C for doses in the range 3-34 dpa. A summary of the tensile data for 9-12Cr ferritic-martensitic steels irradiated under a variety of conditions has been presented by Robertson et al. [3]. Rowcliffe et al. [4] have compared the radiation hardening and deformation behavior of the F82H and HT-9 steels irradiated to low doses at 90 and 250°C. The purpose of the present study is to analyze the radiation-induced microstructural changes occurring in F82H irradiated at temperatures from 90 to 500°C and to identify the distribution of helium produced by doping with <sup>10</sup>B. The objective of this work is to identify the defects responsible for the large increases in yield stress and the loss of strain-hardening capacity induced by neutron irradiation at < 400°C.

Table 1. Chemical Compositions of the Specimens used in this Study (wt%)

Alloys	Cr	C	N	P	S	Al	Si	V	Mn	Ta	W	Total B	<sup>10</sup> B
F82H-std	7.44	0.10	0.002	0.001	0.001	0.019	0.14	0.20	0.49	0.04	2.00	-	-
F82H- <sup>10</sup> B	7.23	0.10	0.002	0.001	0.001	0.021	0.17	0.22	0.50	0.04	2.10	0.0058	0.0058

## 2. Experimental Procedure

The chemical compositions of the specimens used in this study are given in Table 1. The standard F82H steel and the F82H steel doped with  $^{10}\text{B}$  were prepared to examine the effect of helium generation on the microstructures. The specimens were first austenitized at  $1040^\circ\text{C}$  for 30 minutes in a vacuum followed by air-cooling. After that the specimens were tempered at  $740^\circ\text{C}$  for 2 hours in a vacuum followed by air-cooling.

Standard 3 mm-diameter disks punched from 0.25 mm-thick sheet stock were irradiated in the HFIR target in the capsules of HFIR-MFE-JP12 and -JP17 as part of the JAERI/U.S. collaborative program. The exposure for JP-12 was 64904 MWd at 85 MW reactor power and achieved a peak fluence of 57 dpa. The exposure for the JP-17 was 3702 MWd, or approximately 43.6 days at 85 MW reactor power, and the capsule achieved a peak fluence of 3 dpa. The complete description and details of the design, construction, and installation of capsules JP12 [5-8] and JP17 [9-11] have been reported. The irradiation temperatures and displacement damage were  $250^\circ\text{C}$  and 3 dpa for the JP17 capsule and  $300^\circ\text{C}$  and 57 dpa for the JP12 capsule. He generation in the F82H- $^{10}\text{B}$  steel was about 320 appm He at 57 dpa. Microstructures were examined using a JEM-2000FX transmission electron microscope with a  $\text{LaB}_6$  gun operated at 200 kV. Microstructures of unirradiated control specimens were also examined.

## 3. Results

A summary of the radiation-induced defect clusters formed in the F82H steels is presented in Table 2.

Table 2 Summary of Radiation-Induced Defect Clusters Formed in the F82H Steels.

Alloy	Dislocation Loop (no. density, mean size)	Unidentified clusters (no. density, mean size)	MC (no. density, mean size)	$\text{M}_6\text{C}$ (size)	Cavity (no. density, mean size, swelling)	Laths (mean size)
F82H unirradiated			$<1 \times 10^{20} \text{ m}^{-3}$ 14 nm			440 nm
F82H 3 dpa, $250^\circ\text{C}$	$2 \times 10^{22} \text{ m}^{-3}$ 8 nm	$4 \times 10^{23} \text{ m}^{-3}$ 2.9 nm (1-6 nm)	$1 \times 10^{20} \text{ m}^{-3}$ 13 nm		$0 \text{ m}^{-3}$ 0 nm 0%	410 nm
F82H 57 dpa, $300^\circ\text{C}$	$4 \times 10^{22} \text{ m}^{-3}$ 8 nm		$1 \times 10^{21} \text{ m}^{-3}$ 10 nm	3-9 nm	$0 \text{ m}^{-3}$ 0 nm 0%	450 nm
F82H- $^{10}\text{B}$ 57 dpa, $300^\circ\text{C}$	$6 \times 10^{22} \text{ m}^{-3}$ 11 nm		$1 \times 10^{21} \text{ m}^{-3}$ 10 nm	3-9 nm	$2 \times 10^{21} \text{ m}^{-3}$ 2.5 nm 0.002%	440 nm

### 3.1 Initial microstructure of the F82H steel

The microstructure after normalizing and tempering was a lath martensitic structure in the F82H-std steel as shown in Fig. 1(a). The dislocation line density was about  $1 \times 10^{14} \text{ m}^{-2}$ .  $\text{M}_{23}\text{C}_6$  carbides were observed in the matrix and grain boundaries, and the number density and mean size were  $6 \times 10^{19} \text{ m}^{-3}$  and 73 nm, respectively. Only a few MC carbides were observed in the matrix, and the number density and mean size were  $<1 \times 10^{20} \text{ m}^{-3}$  and 14 nm, respectively. The mean width of the lath structure was about 440 nm.

### 3.2 Standard F82H steel irradiated at 250°C to 3 dpa

Figures 1(b) and 1(c) show microstructures of the F82H steel at a low and high magnification, respectively, after irradiation at 250°C to 3 dpa. Dislocation loops formed on {111} planes with  $(a/2)\langle 111 \rangle$  Burgers vectors, and many loops were arranged along dislocation lines, as seen in Fig. 1(c). The number density and mean size of the loops were  $2 \times 10^{22} \text{ m}^{-3}$  and 8.0 nm, respectively. A few MC carbides were observed, and the number density and the mean size were  $1 \times 10^{20} \text{ m}^{-3}$  and 13 nm, respectively. No cavities were found, but some unidentified defect clusters were observed, as shown in Fig. 2. The unidentified clusters cannot be seen in the bright-field image of Fig. 2(a), but they can be observed in Figs. 2(b) and (c) by weak beam dark-field conditions taken with  $g$  or  $2g$  under deviations from the Bragg conditions of  $5g$  excitation. The size of the clusters was 1 - 6 nm (mean size = 2.9 nm), and the number density of the clusters was  $4 \times 10^{23} \text{ m}^{-3}$ . The clusters were very difficult to observe, even in weak beam dark-field conditions excited with a  $5g$  Bragg reflection. The mean width of the lath structure was about 410 nm.

### 3.3 Standard F82H steel irradiated at 300°C to 57 dpa

Figure 3 gives a microstructure of the F82H-std steel irradiated at 300°C to 57 dpa. Many dislocation loops and  $M_{23}C_6$  and MC carbides are seen. The small black contrast seen inside the  $M_{23}C_6$  carbides are  $M_6C$  precipitates, which formed during irradiation, and an example of a dark-field image of the  $M_6C$  precipitates is shown in Fig. 4. The size of the  $M_6C$  particles was 3-9 nm. The mean size and number density of dislocation loops were 11 nm and  $4 \times 10^{22} \text{ m}^{-3}$ , respectively. The loops formed at 300°C and 57 dpa were larger and of higher number density than those at 250°C and 3 dpa. The mean size and number density of MC carbides were 10 nm and  $1 \times 10^{21} \text{ m}^{-3}$ , respectively. No cavities or unidentified defect clusters were observed. The mean width of the lath structure was about 450 nm.

### 3.4 Microstructures of the F82H steels doped with $^{10}B$

Figure 5 shows an example of dislocation loops and cavities formed in the F82H steel doped with  $^{10}B$  irradiated at 300°C to 57 dpa. Number densities of dislocation loops in the doped specimens were higher than in the standard F82H alloy, and the mean size and number density of loops for the F82H- $^{10}B$  were 10.5 nm and  $6 \times 10^{22} \text{ m}^{-3}$ , respectively. Cavities were observed in the matrix and on dislocations. The number density, mean size, and swelling of cavities for the F82H- $^{10}B$  steel were  $2.5 \text{ nm}$ ,  $2 \times 10^{21} \text{ m}^{-3}$  and 0.002%, respectively. The unidentified defect clusters were not observed. The mean width of the lath structure was about 440 nm.

## 4. Discussion

### 4.1 Microstructural development at 250°C

The tensile properties of F82H steel irradiated at 250°C to 3 dpa were published earlier [1]. In spite of the low dose, a large increase in yield strength occurred (Fig. 6). Yielding was followed by severe flow localization and strain softening. These results imply the presence of a high density of defect clusters and/or precipitates which are assimilated or sheared by mobile dislocations, thus giving rise to dislocation channeling. The number density of dislocation loops formed in the F82H steel irradiated at 250°C to 3 dpa was  $2 \times 10^{22} \text{ m}^{-3}$ . The dislocation loops are perfect types of  $\mathbf{b} = (a/2)\langle 111 \rangle$  on {111};  $\langle 100 \rangle$  loops were not observed. In pure iron [12-13] and iron chromium alloys [14-19], the types of dislocation loops observed are  $\mathbf{b} = (a/2)\langle 111 \rangle$  on {111} and/or  $\mathbf{b} = a\langle 100 \rangle$  on {100}. F82H steel is relatively stable during thermal aging at 250°C [20], and essentially no radiation-induced precipitation occurred during the irradiation to 3 dpa at 250°C. The radiation hardening observed at 250°C is therefore primarily associated with the

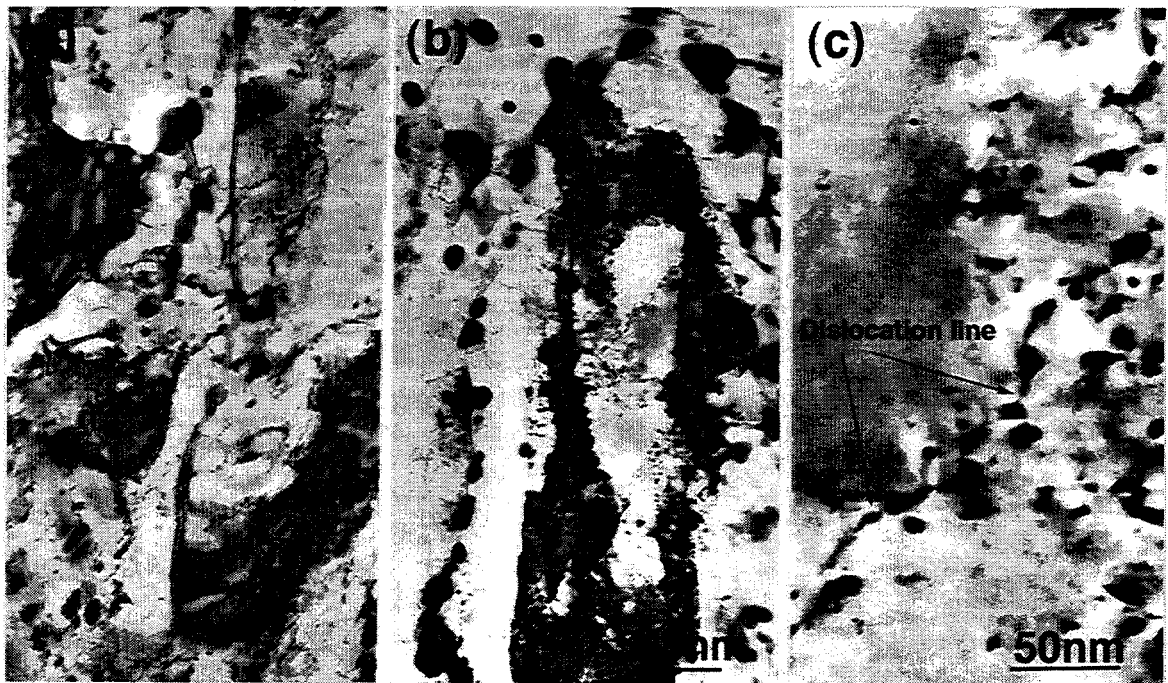


Figure 1. Microstructures of the F82H steel (a) before irradiation, (b), (c) after the 250°C irradiation to 3 dpa, which are at a lower (b) and higher magnification (c), respectively.

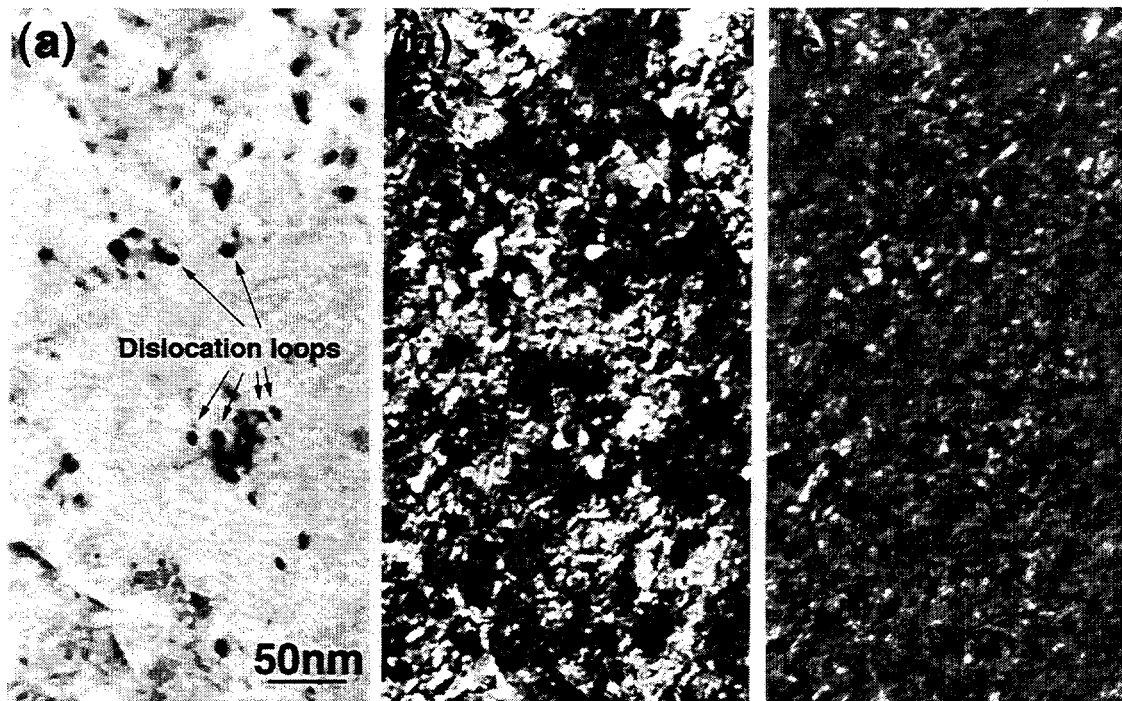


Figure 2. Unidentified defect clusters of the irradiated F82H-std, which are taken by (a) bright-field image, (b) dark-field images of  $g$ , and (c)  $2g$  conditions, under  $s \gg 0$ ,  $g=110$  near 001. The size of the defect clusters is 1 - 6 nm.

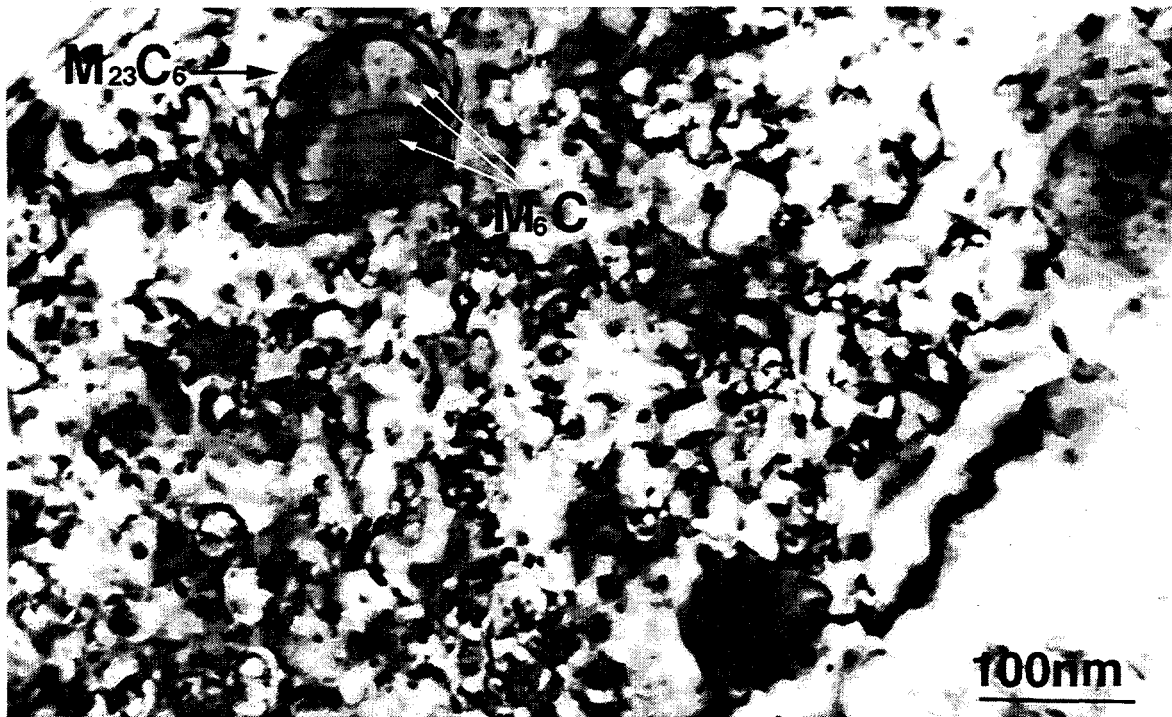


Figure 3. Microstructures in the F82H-std irradiated at 300°C to 57 dpa.

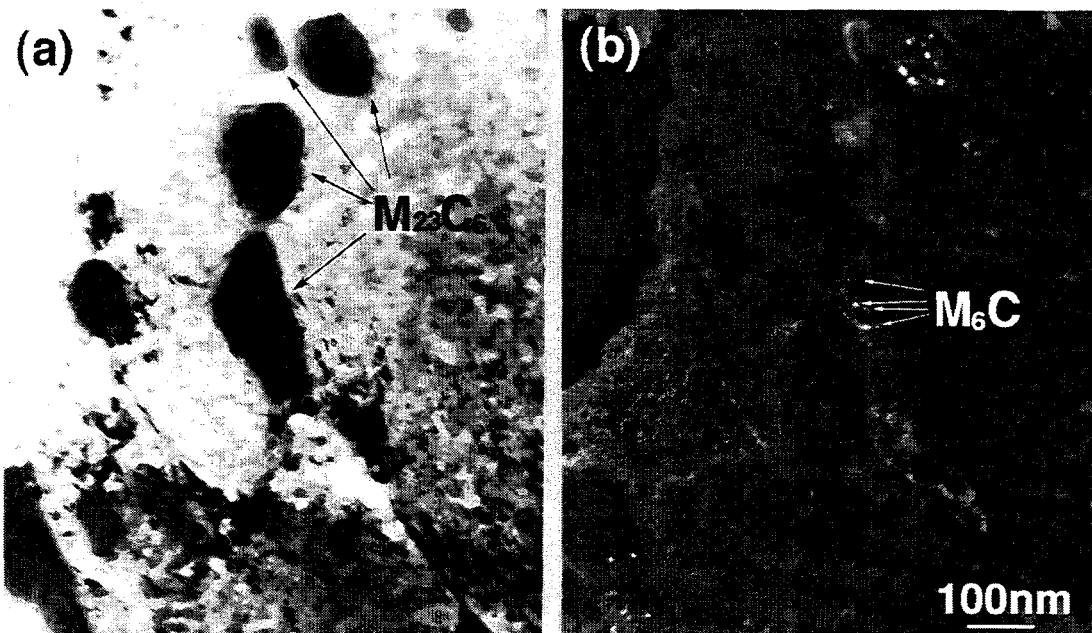


Figure 4. (a) Bright-field image and (b) dark-field image for  $M_6C$  precipitates formed on  $M_{23}C_6$  carbides in the F82H-std irradiated at 300°C to 57 dpa. The size of  $M_6C$  precipitates is 3-9 nm.

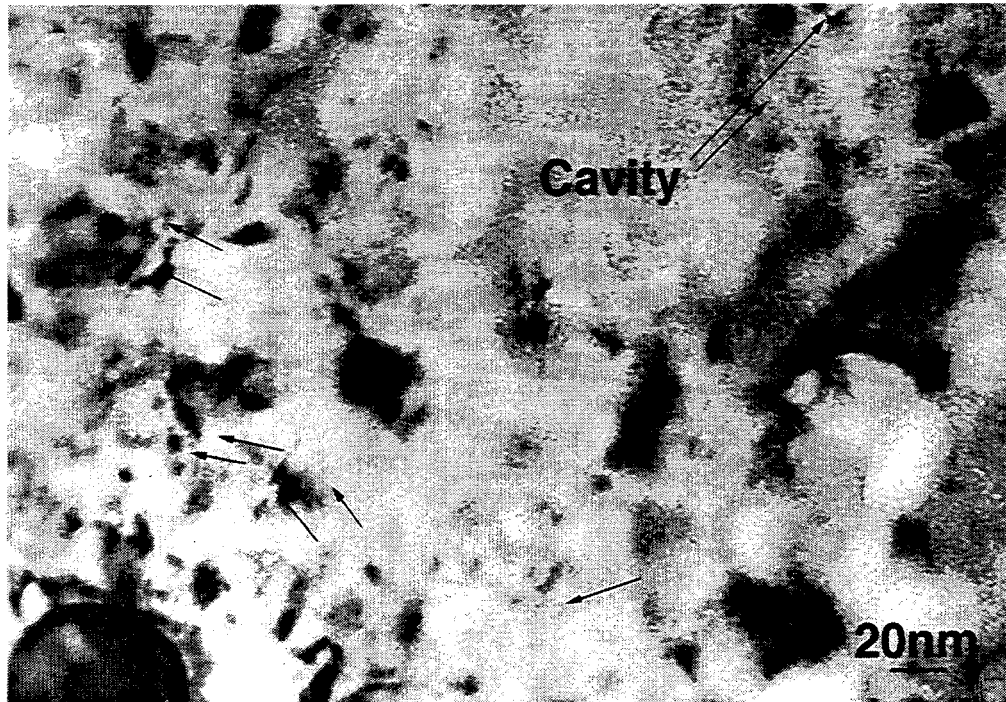


Figure 5. Dislocation loops and cavities formed in the F82H<sup>10</sup>B steel irradiated at 300°C to 57 dpa.

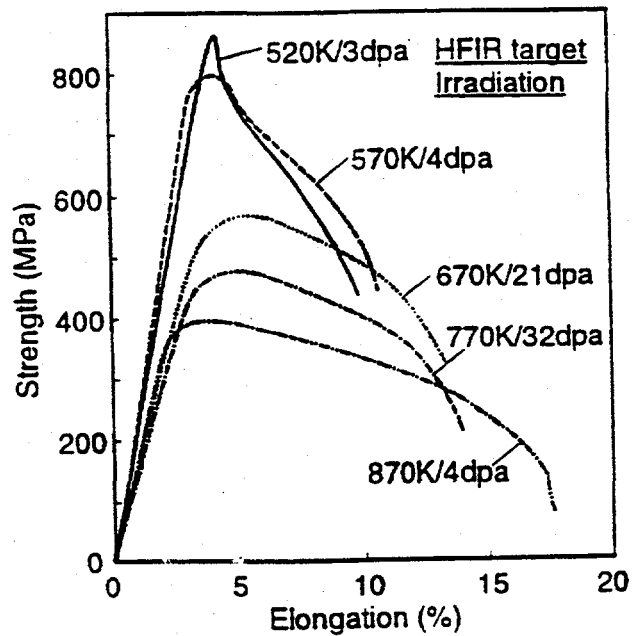


Figure 6. Tensile curves of F82H steel irradiated at temperatures ranging from 250 to 600°C. After ref. [1].

moderate density of  $\langle 111 \rangle$  loops and the high number density of unidentified small defect clusters.

#### 4.2 Microstructural development at 300°C

The tensile behavior at 300°C following irradiation to 4 dpa is very similar to that observed at 250°C. The yield strength is increased to 800 MPa, and plastic instability occurs after a very limited amount of strain hardening. The defect microstructure after irradiation to 57 dpa was dominated by the loops with a number density of  $4 \times 10^{22} \text{ m}^{-3}$ . Interestingly, the small unidentified defect clusters which developed at 250°C could not be detected following the 300°C irradiation to 57 dpa.

A small increase in the number of MC carbides was observed in the F82H steel irradiated up to 57 dpa, but the main change was the  $\text{M}_6\text{C}$  precipitate formation on  $\text{M}_{23}\text{C}_6$  carbides. Thermal aging experiments for the F82H steel showed that no formation of  $\text{M}_6\text{C}$  and MC precipitates was observed below 400°C [20]. In previous irradiation experiments of the F82H steel at temperatures above 420°C to 60 dpa in JMTR, large  $\text{M}_6\text{C}$  precipitates formed in matrix [21]. The formation of  $\text{M}_6\text{C}$  precipitates in the matrix was also observed in 9Cr-1MoVNb and 9Cr-1MoVNb-2Ni steels irradiated at 400°C to 37 dpa in the HFIR, but no formation of  $\text{M}_6\text{C}$  precipitates was observed in the alloys irradiated at 300°C [22, 23]. In those studies, no change of  $\text{M}_{23}\text{C}_6$  phase during the irradiation was observed at  $<500^\circ\text{C}$  [22, 23]. It was mentioned that the  $\text{M}_6\text{C}$  phase was Cr-rich and that Cr supersaturation or segregation during irradiation might play a role for the phase transformation [22, 23]. In another report on several ferritic-martensitic steels (HT9, FV448, and 1.4914),  $\text{M}_6\text{C}$  carbides formed along dislocation lines during irradiation at 460°C to 50 dpa [24]. In the present experiments,  $\text{M}_6\text{C}$  precipitates formed even at 300°C, and the precipitates were not in the matrix, but instead formed on the  $\text{M}_{23}\text{C}_6$  carbides. Judging from these results,  $\text{M}_6\text{C}$  precipitates are likely to form at elevated irradiation temperatures, and the  $\text{M}_6\text{C}$  may be somewhat easier to form in the F82H than in the 9Cr-1MoVNb and the 9Cr-1MoVNb-2Ni steels. The formation mechanism of  $\text{M}_6\text{C}$  precipitates on the  $\text{M}_{23}\text{C}_6$  carbides is not clear, and it may be related to radiation-induced segregation of solute atoms at the surface of  $\text{M}_{23}\text{C}_6$  carbides. Further detailed examination will be necessary to understand it.

#### 4.3 Microstructure of irradiated F82H- $^{10}\text{B}$

The F82H- $^{10}\text{B}$  steel has a higher number density of cavities and dislocation loops than those of the standard F82H steel. Because of the preferential helium-vacancy association, vacancy-interstitial recombination is inhibited relative to that in a steel with little or no helium, and interstitial cluster formation is enhanced.

### 5. Conclusions

Reduced-activation F82H (8Cr-2W-0.2V-0.04Ta) and the F82H steels doped with  $^{10}\text{B}$  were irradiated at 250 and 300°C to 3 and 57 dpa in the HFIR. The microstructures were examined by transmission electron microscopy to explore the relationships between mechanical behavior and microstructure. The results can be summarized as follows:

- (1) The radiation hardening at 250°C is primarily associated with the moderate density ( $2 \times 10^{22} \text{ m}^{-3}$ ) of  $\langle 111 \rangle$  loops and the high number density ( $4 \times 10^{23} \text{ m}^{-3}$ ) of unidentified small defect clusters.
- (2) The defect microstructure after irradiation to 57 dpa at 300°C is dominated by the loops with a number density of  $4 \times 10^{22} \text{ m}^{-3}$ . Interestingly, the small unidentified defect clusters which developed at 250°C could not be detected following the 300°C irradiation to 57 dpa.
- (3) The formation of  $\text{M}_6\text{C}$  precipitates on  $\text{M}_{23}\text{C}_6$  carbides was observed at 300°C to 57 dpa.

- (4) Helium formed from the  $^{10}\text{B}$  during irradiation caused an increase in the number of cavities and dislocation loops that formed.

## ACKNOWLEDGMENTS

The authors would like to thank Dr. S. J. Zinkle of Oak Ridge National Laboratory for fruitful discussions. They are grateful to Messrs. L. T. Gibson, A. T. Fisher, and J. J. Duff, and members of the hot laboratory of ORNL for technical support.

## REFERENCES

1. K. Shiba, I. Ioka, J. P. Robertson, M. Suzuki, and A. Hishinuma, *Euromat-96*(1996), p.265.
2. K. Shiba, unpublished data.
3. J. P. Robertson, R. L. Klueh, K. Shiba, and A. Hishinuma, *J. Nucl. Mater.*, (to be published).
4. A. F. Rowcliffe, J. P. Robertson, K. Shiba, D. J. Alexander, S. Jitsukawa, *J. Nucl. Mater.*, (to be published).
5. R. L. Senn, Fusion Reactor Materials Semiannual Progress Report for Period Ending September 30, 1988, Office of Fusion Energy, DOE/ER-0313/3, p.8.
6. R. L. Senn, Fusion Reactor Materials Semiannual Progress Report for Period Ending March 31, 1988, Office of Fusion Energy, DOE/ER-0313/4, p.7.
7. R. L. Senn, Fusion Reactor Materials Semiannual Progress Report for Period Ending September 30, 1989, Office of Fusion Energy, DOE/ER-0313/5, p.6.
8. J. E. Pawel, K. E. Lenox, A. W. Longest, R. L. Senn, and K. Shiba, Fusion Reactor Materials Semiannual Progress Report for Period Ending September 30, 1994, Office of Fusion Energy, DOE/ER-0313/17, p.3.
9. A. W. Longest, D. W. Heatherly, K. R. Thoms, and J. E. Corum, Fusion Reactor Materials Semiannual Progress Report for Period Ending March 31, 1991, Office of Fusion Energy, DOE/ER-0313/10, p.3.
10. A. W. Longest, D. W. Heatherly, J. E. Wolfe, K. R. Thoms, and J. E. Corum, Fusion Reactor Materials Semiannual Progress Report for Period Ending September 30, 1991, Office of Fusion Energy, DOE/ER-0313/11, p.30.
11. A. W. Longest, D. W. Heatherly, K. R. Thoms, and J. E. Corum, Fusion Reactor Materials Semiannual Progress Report for Period Ending March 31, 1992, Office of Fusion Energy, DOE/ER-0313/12, p.24.
12. A. E. Ward and S. B. Fisher, *J. Nucl. Mater.*, **166**(1989), p.227.
13. E. A. Little, *Rad. Effect*, **16**(1972), p.135.
14. E. Wakai, A. Hishinuma, Y. Kato, S. Takaki, and K. Abiko, *Proc. Ultra High Purity Base Metals*, Eds. K. Abiko, K. Hirokawa, and S. Takaki, The Japan Institute of Metals Sendai (Japan), (1994), p.522.
15. E. Wakai, A. Hishinuma, T. Sawai, S. Kato, S. Isozaki, S. Takaki, and K. Abiko, *Phys. Stat. Sol. (a)*, **160** (1997), p.441.
16. Y. Katoh, A. Koyama, and D. S. Gelles, *J. Nucl. Mater.*, **225**(1995), p.154.
17. D. S. Gelles, *J. Nucl. Mater.*, **225**(1995), p.163.
18. S. Ohnuki, H. Takahashi, and T. Takeyama, *J. Nucl. Mater.*, **122&123**(1984), p.317.
19. T. Muroga, A. Yamaguchi, and N. Yoshida, *Effects of Radiation on Materials: 14th International Symposium*, vol. 1, ASTM STP **1046**(1989), p.396.
20. K. Shiba, unpublished data.
21. T. Shibayama, A. Kimura, and H. Kayano, *Euromat-96*(1996), p.533.
22. P. J. Maziasz, *J. Nucl. Mater.*, **169**(1989), p.95.
23. P. J. Maziasz, R. L. Klueh, and J. M. Vitek, *J. Nucl. Mater.*, **141-143** (1986), p.927.
24. P. Dubuisson, D. Gilbon and J. L. Seran, *J. Nucl. Mater.*, **205**(1993), p.178.